Cyclodextrin reduces cholesterol crystal-induced inflammation by modulating complement activation

Running title: Cyclodextrin inhibits CC-induced complement activation

Siril S. Bakke [*, 1], Marie H. Aune [*, 1], Nathalie Niyonzima[*, 2], Katrine Pilely[†, ‡, 2], Liv Ryan[*], Mona Skjelland[§], Peter Garred[†, ‡], Pål Aukrust[¶, ‖, #, **], Bente Halvorsen[¶, ‖, #], Eicke Latz[*,††], Jan K. Damås[*], Tom E. Mollnes[*, #, ‡‡, §§, ¶¶] and Terje Espevik[*]

[*] Norwegian University of Science and Technology, Centre of Molecular Inflammation Research, and Department of Cancer Research and Molecular Medicine, Trondheim, Norway

[†] Laboratory of Molecular Medicine, Department of Clinical Immunology, Section 7631 Rigshospitalet, Copenhagen, Denmark

[‡] Faculty of Health and Medical Sciences, University of Copenhagen, Copenhagen, Denmark

[§] Department of Neurology, Oslo University Hospital Rikshospitalet, Oslo, Norway

[¶] Research Institute of Internal Medicine, Oslo University Hospital Rikshospitalet, Oslo, Norway

[‖] Institute of Clinical Medicine, Faculty of Medicine, University of Oslo, Oslo, Norway

[#] K.G. Jebsen Inflammation Research Center, University of Oslo, Oslo, Norway

[**]Section of Clinical Immunology and Infectious Diseases, OUS Rikshospitalet, Oslo, Norway

[††] Institute of Innate Immunity, University Hospitals Bonn, Bonn, Germany

[‡‡] Department of Immunology, Oslo University Hospital Rikshospitalet, and University of Oslo, Oslo, Norway

[§§]Research Laboratory, Nordland Hospital, Bodø, Norway

[¶¶]K.G. Jebsen TREC, Institute of Clinical Medicine, University of Tromsø, Tromsø, Norway

[1]SSB and [1]MHA contributed equally to this work, [2]NN and [2]KP contributed equally to this work.

Footnotes

1. Corresponding author and address: Prof. Dr. Terje Espevik

Phone number: 0047 72825337, Fax: 0047 72571463

E-mail: terje.espevik@ntnu.no

Norwegian University of Science and Technology – NTNU,

Department of Cancer Research and Molecular Medicine,

Centre of Molecular Inflammation Research

Post box 8905, N-7491 Trondheim, Norway

2. Grant support:

This work was supported by the Research Council of Norway through its Centre's of Excellence funding scheme, project number 223255/F50 (TE), the European Community's Seventh Framework Programme under grant agreement n°602699 (DIREKT) (TEM), The Norwegian Council on Cardiovascular Disease (TEM), The Odd Fellow Foundation (TEM) and Danish Heart Foundation (16-R107-A6650-22966) (KP and PG) and the Danish Research Council for Independent Research (DFF – 6110-00489) (KP and PG). The Norwegian Council on Cardiovascular Disease [NCCD-2014]; The Odd Fellow Foundation [OFF-2014]; and the European Community's Seventh Framework Programme under grant agreement n° 602699 (DIREKT) (TEM).

3. Nonstandard Abbreviations and Acronyms:

BCD	(2-Hydroxypropyl)-β-cyclodextrin
CC	cholesterol crystals
CVID	common variable immunodeficiency
CR1 and 3	complement receptor 1 and 3
MASP	mannose-binding lectin serine protease
MSU	monosodium urate
NLRP3	nod-like receptor pyrin domain containing 3
ROS	reactive oxygen species
TCC	terminal complement complex

Abstract

Cholesterol crystals (CC) are abundant in atherosclerotic plaques and promote inflammatory responses via the complement system and inflammasome activation. Cyclic oligosaccharide 2-hydroxypropyl-β-cyclodextrin (BCD) is a compound that solubilizes lipophilic substances. Recently we have shown that BCD has an anti-inflammatory effect on CC via suppression of the inflammasome and liver-X-receptor activation. The putative effects of BCD on CC-induced complement activation remain unknown. Here we found that BCD bound to CC and reduced deposition of immunoglobulins, pattern recognition molecules and complement factors on CC in human plasma. Furthermore, BCD decreased complement activation as measured by terminal complement complex (TCC) and lowered the expression of complement receptors on monocytes in whole blood in response to CC exposure. In line with this, BCD also reduced reactive oxygen species formation caused by CC in whole blood. Furthermore, BCD attenuated the CC-induced pro-inflammatory cytokine responses (e.g. IL-1α, MIP-1α, TNF, IL-6, and IL-8) as well as regulated a range of CC-induced genes in human peripheral blood mononuclear cells. BCD also regulated complement-related genes in human carotid plaques treated *ex vivo*. Formation of TCC on other complement activating structures like monosodium urate crystals and zymosan was not affected by BCD. These data demonstrate that BCD inhibits CC-induced inflammatory responses, which may be explained by BCD-mediated attenuation of complement activation. Thus, these findings support the potential for using BCD in treatment of atherosclerosis.

Introduction

Atherosclerosis is characterized by a bidirectional interaction between lipids and inflammatory mechanisms that in some degree could be modulated by statins. (1). However, statins may fail to improve cardiovascular outcome in some patients (2-4), and it is a global priority to find new, efficient and cheap treatments for atherosclerotic disorders. Atherosclerosis is also considered a chronic or non-resolving inflammatory reaction where the mechanisms behind triggers of plaque inflammation have not yet been fully elucidated. Studies during the last decade, however, establish cholesterol crystals (CC) as an important trigger of inflammatory responses during development of atherosclerosis. It is believed that CC contribute to the pathogenicity by fueling chronic inflammation in the plaques (5) through activation of the NOD-like receptor pyrin domain containing 3 (NLRP3) inflammasome (6-8). Thus, one strategy for treatment and prevention of atherosclerosis, is to inhibit the early inflammatory response to CC, which constitutes a characteristic hallmark of atherosclerosis (9).

The complement system plays a critical role in the development of atherosclerosis (10) including its ability to mediate CC-induced inflammation (8). The pattern recognition molecule C1q is the initiator of the classical pathway (CP) of complement and binds to the CC surface, resulting in downstream complement activation, opsonization and formation of the terminal complement complex (TCC) (8). Reactive oxygen species (ROS) and pro-inflammatory cytokines are generated from monocytes and granulocytes that have phagocytosed CC (8). Pattern recognition molecules of the lectin pathway (LP) include mannose-binding lectin (MBL) and the ficolins. Recently, we found that CC can activate both the CP and LP through C1q, MBL and ficolin-2 (11). The CP, LP and alternative complement pathways merge at C3, leading to cleavage of C3 to C3a and C3b, with subsequent cleavage of C5 to C5a and C5b, the latter leading to the assembly of the TCC complex (C5b-C9). In

addition, C3a and C5a are themselves potent anaphylatoxins that induce potent inflammatory responses (12, 13).

The cyclic oligosaccharide 2-hydroxypropyl-β-cyclodextrin (BCD) is commonly used for drug delivery to improve solubility, bioavailability and stability (14). In addition, it is used as treatment of the lysosomal storage disease Niemann-Pick Type C (15-17), and is therefore FDA-approved and has been shown to be safe in several species (18-20). Recently we showed that BCD is effective in both preventing and treating atherosclerosis in a mouse model (21). The beneficial effects of BCD on atherogenesis include decreasing lesion size, lowering the CC burden, promoting plaque regression, increasing reverse cholesterol transport and decreasing systemic inflammation. The mechanism proposed is that BCD initiates production of oxysterols in cells and hence activates the liver X receptor (LXR) and this was shown in mouse macrophages and in human carotid plaques. This reprograms cells to an anti-inflammatory state together with a more active cholesterol efflux resulting in less free cholesterol in the cells (21). As BCD is reported to bind to CC (21) we hypothesized that BCD may also inhibit CC-induced inflammatory responses by inhibiting complement activation.

We found that BCD decreased deposition of IgA, IgM and complement factors on the CC surface and reduced complement activation. In accordance with this, BCD reduced CC-induced ROS and pro-inflammatory cytokine release from human PBMC. Moreover, BCD was a critical regulator of inflammation and complement related gene expression in PBMC and in human carotid plaques. These observations suggest that BCD affects upstream complement activation that may attenuate inflammation in atherosclerosis.

Materials and methods

Reagents

Cells were isolated with Polymorphprep™ (Axis-Shield). Lepirudin/Refludan® (Celgene) was used as an anticoagulant in whole-blood experiments. CC were prepared as described before, and kept in 0.05 % HSA/PBS (8). BCD was kindly provided by CTD Holdings. Ultrapure cholesterol and zymosan were from Sigma-Aldrich, heat-aggregated human IgG and human serum albumin (HSA) were from Octapharma. RNeasy micro- or minikit from Qiagen), nCounter ® analysis system and nCounter GX Human Immunology Kit v1 and v2 was supplied from Nanostring Technologies. Barbital buffer contained 5 mM barbital natrium, 145 mM NaCl, 2 mM $CaCl_2$, and 1 mM $MgCl_2$ at pH 7.4. C3-inhibitor compstatin analog 22 CP20 from (22) and CP40 were kindly provided as a gift from Dr. John Lambris. Human immunoglobulin (Pentaglobin ® (76 % IgG, 12 % IgA, 12 % IgM)) was provided by Biotest. FACS lysing solution was from BD Biosciences (349202) and Erythrocyte-lysing Reagent from DAKO (Easy-Lyse, S2364). FAM FLICA *in vitro* Caspase detection kit was purchased from Immunochemistry Technologies, and PHAGOBURST from BD Biosciences. The following antibodies were used: PE mouse anti-rabbit IgG detector (BD 558553), FITC-rabbit anti-mouse immunoglobulin (DAKO F0261), FITC goat anti-mouse IgGAM (BD349031), A488 Goat anti-mouse IgG (A11001, Life Technologies), mouse IgG2a κ (BD 553454), mouse IgG1κ (BD 349040), PE mouse IgG1 κ (BD 559320), rabbit IgG (R&D AB105-C), rabbit anti-human C1q (A0136, Dako), rabbit anti-human C3c Complement (F0201, DAKO), mouse anti-complement component C5b-9 (DIA 011-01, Antibodyshop), FITC-goat anti-human IgM (F53384, Sigma-Aldrich), FITC-goat anti-human IgA (F5259, Sigma-Aldrich), PE-mouse anti-human IgG (BD 444787), PE-mouse anti-human IgG (BD 555787), FITC-goat anti-human IgGAM (Sigma F6506), PE-mouse anti-human CD35 (Biolegend 333405), Brilliant Violet 605™-mouse anti-human CD11b antibody (Biolegend

301331), FITC-mouse anti-human CD14 (MφP9, BD 345784), PE-mouse anti-human CD11b (BD 333142), FITC-goat anti-rabbit antibody (F1262, Sigma-Aldrich), FITC-goat anti-mouse antibody (F0479, DAKO), rabbit IgG isotype control (Invitrogen), and mouse anti-human C1q clone 85 (IgG1) (MW1828, Sanquin). In house produced monoclonal antibodies: mouse anti-human ficolin-2 FCN219 (IgG2a) (23) and an inhibitory mouse anti-human ficolin-2 FCN212 (IgG1κ) (24).

Whole blood assay and human cells

The whole blood assay was performed as described before (25). Briefly, whole blood was anticoagulated with lepirudin (Refludan; Celgene) before inhibitors/stimuli diluted in PBS were added and incubated at 37°C under constant rotation. Samples were added CC (1 mg/ml), BCD (10 mM), compstatin (20 μM) or HSA/PBS unless otherwise stated. Plasma was isolated by centrifugation from untreated lepirudin whole blood, and stored at -20°C before use in experiments. Plasma from a patient with common variable immunodeficiency (CVID) had the following values for the immunoglobulins: IgG 3.6 mg/ml (reference 8-16 mg/ml), IgA 0.5 mg/ml (reference 0.6-3.5 mg/ml) and IgM <0.1 mg/ml (reference 0.4-3 mg/ml). For the serum samples, venous blood from healthy donors was collected in dry glass vials with no additive, and left for 2 h at room temperature for coagulation. Serum was collected by centrifugation (2500g for 15 min) and stored at -80°C until use. Human PBMC were isolated from whole blood using polymorphprep according to the manufacturer's instructions. PBMC were kept in 50 % autologous plasma and pretreated with BCD (10 mM) or PBS for 1 h before adding CC (2 mg/ml) or HSA/PBS for 5 or 0.5 h. Cells were lyzed in RLT buffer with 1 % betamercapotethanol for RNA isolation and supernatant was collected for multiplex cytokine assay measurement.

Human atherosclerotic carotid plaques

Data used were reanalyzed from already published results (21). In short, patients with high-grade internal carotid stenosis (≥70%) and ischemic stroke within the last month or >1 month ago were recruited at Department of Neurology, Oslo University Hospital Rikshospitalet. Biopsies from atherosclerotic carotid plaques, obtained from patients, were placed in Dulbecco's modified Eagle's medium (D-MEM/F12; Gibco) enriched with 30 mg/ml endotoxin free and fatty acid free bovine serum albumin (Sigma). The biopsies containing atherosclerotic plaques of each patient were split into macroscopically equal pieces and incubated for 16 h with 10 mM BCD or PBS and placed in RNA Later (Qiagen) for RNA analysis. Homogenization was performed with a FastPrep® 24 instrument (≈6 m/s, MD Biomedicals) three times 40 seconds with zirconium oxide beads (Bertin Tech) (six 2.8 mm beads and 0.8 g 1.4 mm beads per sample) in Isol-RNA Lysis Reagent (VWR, 5Prime). The aqueous phase was isolated after adding chloroform and centrifugation (13000 rpm, 15 min, 4°C) and RNA was isolated further with RNeasy microkit (Qiagen).

Complement activation assessment

Plasma from whole blood of healthy donors was diluted 6x in PBS and incubated with BCD (5 and 10 mM) or PBS for 30 minutes at 37°C in the presence of HSA/PBS, CC (0.5-1 mg/ml) or MSU (0.25 mg/ml). Plasma from a immunodeficient patient was diluted 6x and incubated with BCD (10 mM) or PBS for 30 minutes at 37°C in the presence of CC (1 mg/ml) or HSA/PBS. A mixture of zymosan (10 mg/ml) and heat aggregated human IgG (Octapharma AB, 10 mg/ml) was used as a positive control for complement activation. TCC in the fluid phase was measured by ELISA as described elsewhere (26). In the deposition experiments, plasma was diluted in PBS and incubated with HSA/PBS or CC (1 mg/ml), in the presence or absence of BCD (10 and 20 mM), compstatin CP20 or CP40 (10 and 20 μM)

or a mixture of the IgG, IgM and IgA (1.3 mg/ml Pentaglobin) for 30 minutes at 37°C and the reaction was stopped by adding EDTA (10 mM). CC were stained for IgGAM, IgG, IgA, IgM, C1q, ficolin-2, C3c or TCC for 30 minutes. IgGAM staining detects all three immunoglobulins. The anti-TCC monoclonal antibody (aE11) detects a neoepitope expressed in C9 when incorporated into the TCC complex. For detection of ficolin-2 deposition on CC no EDTA was used, and plasma was diluted in barbital buffer with 0.5% FCS. Antibody staining was measured on a BD FACSCanto II (BD Biosciences). To investigate the binding of C1q and ficolin-2 to CC, serum was added to CC with or without BCD (10 mM) in barbital buffer with 0.5% BSA, with or without ficolin-2 inhibitory antibody (10 μg/ml), C1q inhibitory antibody (10 μg/ml) or isotype control antibody for 30 minutes at 37°C rolling. Antibody staining was measured on a Gallios flow cytometer (Beckman Coulter). All data were analyzed using FlowJo V10 (Tree Star) and 7.6. All CC populations were gated using auto-gating function in FlowJo (at least 80 % of the events present). Control for IgM, IgA and IgGAM experiments were FITC- goat anti-mouse IgGAM, and for the rest of the experiments isotype controls were used.

Phagocytosis, CR3 and CR1 expression

CC (1 mg/ml) or PBS were pre-incubated with BCD (10 mM), compstatin CP40 (20 μM) or PBS for 15 min, then incubated with whole blood for 30 min at 37°C. Cells were fixed and red blood cells lysed with lysing solution for 15 min in room temperature, and then stained with anti-CD14-FITC, anti-CD11b-BV605, anti-CD35-PE for 15 min in room temperature. The samples were run on a LSR II flow cytometer (BD Biosciences) and analyzed with FlowJo (version 10.1, Tree Star). Gating was performed on scatter-CD14 flow cytometric dot plots where the monocyte population was defined as $CD14^{+(high)}$ and the granulocyte

223 population was defined as $CD14^{+ (medium)}$. Phagocytosis was determined based on shift in side
224 scatter induced by CC ingestion and negative control was gated so that less than 1-3% of the
225 events are positive. CR3 (CD11b) and CR1 (CD35) expression were measured as median
226 fluorescence intensity (MFI).

227

228 **Reactive oxygen species production**

229 Reactive oxygen species (ROS) was detected using the oxidative burst test Phagoburst,
230 following the manufacture's protocol with some modifications. CC (1 mg/ml) or PBS were
231 pre-incubated with BCD (10 mM), compstatin CP40 (20 μM) or PBS for 15 min, then
232 incubated with whole blood for 10 min at 37°C, after which DHR 123 substrate was added for
233 10 min. Red blood cells were lysed with FACS lysing solution for 15 min at RT, and the cells
234 were washed and incubated with anti-CD14-PE for 15 min at RT. The samples were run on a
235 LSR II flow cytometer (BD Biosciences) and analyzed with FlowJo (version 10.1, Tree Star).
236 Gating was performed on scatter-CD14 flow cytometric dot plots where the monocyte
237 population was defined as $CD14^{+(high)}$ and the granulocyte population was defined as $CD14^{+}$
238 $^{(medium)}$.

239

240 **Caspase-1 activation detection**

241 FAM FLICA in vitro Caspase-1 detection kit was used. CC (1 mg/ml) or PBS were pre-
242 incubated with BCD (10 mM), compstatin CP40 (20 μM) or PBS for 15 min, and then
243 incubated with whole blood for 4 h and incubated for 2 h with FLICA probes for caspase-1
244 detection. Blood was stained with anti–CD14-PE for 15 min at RT before red blood cells lysis

with Erythrocyte-lysing Reagent for 20 min at RT. Analysis was performed on a BD FACSCanto II (BD Biosciences). Data were analyzed with FlowJo (version 10.1, Tree Star). Gating was performed on scatter-CD14 flow cytometric dot plots where the monocyte population was defined as $CD14^{+(high)}$ and the granulocyte population was defined as $CD14^{+(medium)}$.

Gene expression and bioinformatic analysis

RNA expression analysis was run on the nCounter ® analysis system, running 12 samples at a time (one strip). The procedure was performed according to the manufacturer´s instructions, applying about 100 ng mRNA. Kit used for PBMC was a fixed codeset for mRNA analysis with genes involved in human immunology nCounter GX Human Immunology Kit v1 and v2 (Nanostring Technologies). Kit used for plaques was a fixed codeset for mRNA analysis, nCounter GX Human Immunology Kit v2 (Nanostring Technologies), spiked with another 30 probes (nCounter Panel Plus, (21)). Number of mRNA molecules per gene was accounted for detection level (mean negative controls + 2 standard deviation of negative controls), and normalized against instrument variations (positive controls) and housekeeping genes found to be stable (for PBMC G6PD, OAZ1, RPL10, POLR2A, HPRT1 and for plaques RPL19, EEF1G, TUBB, OAZ1, GAPDH, POLRA2, G6PD, HPRT1) using NSolver Analysis Software 2.5.34 (Nanostring Technologies). The data was imported into Partek Genomics Suite 6.6, and the data was 2 log transformed and batch-corrected for the donor variations (PBMC) and for the interaction strip and patient (Plaques). For PBMC, a gene list was prepared merging genes involved in the Cytokine-cytokine receptor interaction (kegg map 04060) and Chemokine signaling pathway (kegg map 04062) and BCD effect on the CC-induced genes were presented as a volcano plot with fold change and p-values obtained from the ANOVA. Pathway enrichment analysis was performed in Partek Pathway for the plaque

data (Fishers exact test), and gene expression of genes relevant for complement cascade was illustrated in Adobe Illustrator 18.0.0 with fold changes obtained from the ANOVA.

Measurement of cytokine release

Supernatants from PBMC were analyzed according to the manufacturer's instructions by multiplex cytokine assay (Bio-Plex; Bio-Rad Laboratories Inc.) for IL-1α, IL-1β, IL-6, IL-8/CXCL8, monocyte chemotactic protein/chemokine ligand 2 (MCP-1/CCL2), macrophage inflammatory protein/ chemokine ligand 3 (MIP-1α/CCL3) and tumor necrosis factor (TNF).

Statistics

GraphPad Prism version 5.03 (Graphpad Software) was used for analysis, and $p<0.05$ was considered statistically significant. Data are expressed as mean ± SEM. For statistical analysis, two-way ANOVA with Bonferroni post-test were employed in Fig. 1A and Supplemental Fig. 2, repeated measures ANOVA with Dunnett's multiple comparisons test was used in Fig. 2 C-D, and Wilcoxon matched pair signed rank test was used in Fig. 5 and Fig. 6. Gene expression and multiplex cytokine assay was analyzed with Partek Genomics Suite 6.6 using ANOVA models.

Study approval

Approval no. 2009/2245 was received from the Regional Committee for Medical and Health Research Norway for the whole blood experiments, and approval no. 2009/2259 for the carotid plaques. Plasma from the immunodeficient patient was obtained and used in accordance with a protocol approved by the Regional Committee for Medical and Health Research Norway (2015/419). The regional health ethics committee in the Capital Region of

Denmark (H2-2011-133) has approved the serum experiments. The study complies with the principles outlined in the Declaration of Helsinki for use of human tissue or subjects. Signed informed consent for participation in the study was obtained from all individuals.

Results

BCD inhibits CC-induced complement activation

Previously we have shown that CC initiate an inflammatory response through activation of the complement system (8). We therefore first evaluated if BCD affected CC-induced complement activation. The results revealed that BCD specifically and significantly decreased CC-induced complement activation as assessed by a marked decrease in TCC generation in human plasma (Fig. 1A). Moreover, deposition of TCC on CC surface was reduced with BCD treatment (Fig. 1B). Likewise, binding of C3c to CC was inhibited by BCD treatment (Fig. 1C). At 10 mM concentration, which is a subtoxic dose (21), BCD was not as effective as the C3 inhibitor compstatin (20 μM) to inhibit depositions of TCC and C3c on CC (Fig. 1B-C). However, by increasing the dose to 20 mM the inhibitory effect of BCD was more comparable with the effect of compstatin (Supplemental Fig. 3A-D).

It has previously been reported that a 6 h incubation of CC with BCD will dissolve the crystals (21). We did not observe dissolution of the CC by BCD at 30 min, indicating that the effects observed on complement in the early stages of response to CC in plasma are not due to crystal dissolution (Supplemental Fig. 1).

BCD prevents deposition of complement pattern recognition molecules on CC

316 Complement activation is initiated by binding of pattern recognition molecules to targets (8,
317 11). Deposition of C1q and ficolin-2 on CC was measured in plasma or serum in the presence
318 or absence of BCD or specific inhibitory antibodies for 30 min. Deposition of C1q and
319 ficolin-2 on the surface of CC was reduced in presence of BCD (Fig. 2A-B), similar to the
320 specific inhibitory antibodies to C1q or ficolin-2 (Fig. 2C-D). In contrast, BCD had no effect
321 on MBL binding to CC in serum or plasma (data not shown).

322

323 **IgA and IgM bind to CC and BCD prevents their depositions on CC surface**

324 Complement activation is also initiated by binding of immunoglobulins to target surfaces
325 (11), most likely through interaction with the pattern recognition molecules. We first assessed
326 the ability of native IgA, IgG or IgM to bind to CC. The results revealed that, in human
327 plasma, IgM and IgA, but not IgG, were detected on the CC surface (Fig. 3A-C).
328 Furthermore, deposition of IgA and IgM (Fig. 3D-E) on CC was markedly lower in plasma of
329 a CVID patient, than in the healthy donor. The binding of IgM and IgA to the CC surface
330 (Fig. 3D-E) was restored by reconstitution of plasma with Pentaglobin (a mixture of IgG, IgA
331 and IgM) that resulted in a 2.6-fold increase in the IgM concentration in the plasma from this
332 patient. TCC formation in response to CC and zymosan-IgG was greatly reduced in the
333 plasma of a CVID patient in comparison to plasma from healthy individuals (Fig. 3F). This
334 response was also restored by reconstitution of plasma with Pentaglobin (data not shown).
335 Since BCD binds to the CC surface, we wanted to see whether the inhibitory effect of BCD
336 on CC-induced complement was due to this compound affecting Ig deposition on CC. IgM
337 and IgA detected on CC were reduced by BCD in human plasma (Fig. 4A-C), but no
338 reduction in IgM deposition was observed for compstatin (Supplemental Fig. 3E, F). These

results demonstrate that binding of IgM and/or IgA to CC is essential for complement activation initiated by CC, and that BCD inhibits IgA and IgM deposition onto CC.

BCD reduces CC-induced increase in surface expression of phagocytic receptors on monocytes

The initiation of the complement cascade after CC exposure leads to phagocytosis of CC (8). Complement receptor 3 (CR3 or CD11b/CD18) recognizes mainly iC3b, while complement receptor 1 (CR1, CD35) recognizes C3b and C4b, and together they promote phagocytosis. Having observed a strong inhibition of complement deposition on CC by BCD, we next assessed whether BCD also reduced phagocytosis of CC. Addition of CC to whole blood resulted in phagocytosis of CC by monocytes and granulocytes, however we found that phagocytosis of CC was not reduced by BCD (Fig. 5A-B). Surprisingly, BCD gave an increase in CC phagocytosis in granulocytes (Fig. 5B). Expression of CR1 and CR3 on the cell surface was increased by CC and BCD significantly decreased both receptors in monocytes, but not in granulocytes (Fig. 5C-F). These results indicate that BCD affects phagocytic receptor expressions in monocytes in response to CC exposure.

BCD inhibits CC-induced ROS production

Our recent findings show that phagocytosis of CC leads to reactive oxygen species (ROS) and active caspase-1 in a complement dependent manner (6, 8). CC-induced ROS production and caspase-1 activity was assessed in the presence or absence of BCD in granulocytes and monocytes in whole blood. BCD reduced the CC-induced ROS formation in both monocytes and granulocytes (Fig. 6A-B). BCD had only minimal effect on CC-induced caspase-1

activity (Fig. 6C-D). These results demonstrate that BCD inhibits ROS production, which may affect CC-induced inflammasome activation.

To evaluate if any of the effects observed was due to cytotoxic responses of the substances used, whole blood was incubated with CC with or without BCD at maximum incubation time (6 h) to examine cytotoxicity. The results revealed that none of the substances in the concentrations used in this study were cytotoxic for blood cells (Supplemental Fig. 2).

BCD modifies CC-induced gene expression and reduces cytokine release in PBMC

The ability of CC to activate complement results in the release of multiple cytokines and chemokines from the human blood cells (8). Having observed a strong inhibition of BCD on CC-induced complement, we examined the effect of BCD on gene expression induced by CC in human PBMC. PBMC were isolated from whole blood, incubated with CC for 5 h in the presence or absence of BCD, and gene analysis of immunology related genes involving cytokine-cytokine receptor interaction and chemokine signaling pathway were performed. These data revealed that BCD affected gene expressions of a range of CC-induced chemokines and cytokines and their related genes (Fig. 7A). A number of key genes that regulates inflammatory responses to CC including inflammasome-dependent pro-inflammatory cytokine IL-1β, and other key genes such as IL-6 and IL-1α were significantly reduced upon exposure to BCD. CC-induced mRNA expression of TNF was reduced by BCD, but did not reach statistical significance (FC=-1.6, $p=0.06$). In addition, genes related to the NLRP3 pathway including the NLRP3 sensor (FC=-2.3, $p=0.08$) and caspase-1 (FC=-1.5, $p<0.05$) were also reduced by BCD treatment. On the other side, BCD significantly inhibited CC induced mRNA expression of TNF (FC=-1.7, $p=0.02$) and NLRP3 (FC=-1.7, $p=0.01$) after 30 min of CC exposure (data not shown).

We next tested the effect of BCD on cytokines and chemokines initiated by CC in PBMC. Addition of CC to PBMC for 5 h resulted in a significant ($p<0.05$) release of pro-inflammatory cytokines and chemokines including IL-1β, TNF, IL-1α, IL-6, MIP-1α, while IL-8 was slightly increased, but did not reach statistical significance ($p=0.06$) (Fig. 7B, Supplemental Table 1). However, once exposed to BCD, CC-induced secretion of TNF, IL-8, MIP-1α, IL-1α and IL-6 were significantly reduced ($p<0.05$). The reduction in IL-1β did not reach significance ($p=0.08$). However, a stronger BCD effect on IL-1β release occurred at an earlier time point as BCD significantly reduced IL-1β release after 30 min of CC exposure ($p<0.05$, Supplemental Table 1).

BCD *ex vivo* treatment of carotid plaques affects the expression of genes in the complement cascade

Atherosclerotic plaques are known to contain CC as a part of their inflammatory milieu and CC in very early atherosclerotic lesions are suggested to fuel the inflammation in the plaques (5). Data were reanalyzed from already published results (21) where human carotid plaques were incubated *ex vivo* in presence or absence of BCD and mRNA was isolated and gene profiling in immunology related genes were performed. When taking into consideration genes changed with BCD treatment, a pathway analysis revealed a significant enrichment for the pathway "Complement and coagulation cascades" (kegg map 04610, $p<0.05$). Visualizing this pathway, revealed that many of the genes involved in the complement system were affected by BCD to a lesser or higher degree, in particular the increase in C3 and decrease in C5 expressions (Fig. 8). The reanalysis of these data (21) suggest that BCD may affect the development of atherosclerosis in human carotid plaques through modulating complement activation.

Discussion

BCD is an oligosaccharide that solubilizes lipophilic substances and is commonly used in pharmaceuticals (18-20). We have previously shown that CC, abundant in atherosclerotic plaques, initiate an inflammatory response via complement- and NLRP3 inflammasome activation (8). Recently we have shown that BCD has an anti-inflammatory effect on CC in atherosclerotic plaques (21). Here we have found that initiation of complement activation on the CC surface starts with IgM, ficolin-2 and C1q that bind to CC within 30 min, in agreement with previous findings (8, 11). In addition, depletion of C1q was previously shown to reduce CC-induced TCC formation, indicating a strong role for the CP (8, 11). C1q has been observed to bind directly and indirectly via IgM to the CC surface (11), however, whether C1q also can bind via IgA remains unknown. Based on previous data from Pilely et al. it is clear that in the presence of IgM antibodies C1q is superior in activating complement on the CC compared to the lectin pathway (11). Ficolin-2 may exerts its main role when antibodies are not present and may function as an opsonin for phagocytosis independent of complement activation. Furthermore, we found that also IgA bound to the CC in human plasma and the ability of IgA to activate the complement system was originally thought to occur mainly via the alternative pathway of complement. However more recent studies indicate that lectin pathway is the initiating key event (27), but the biological importance is unknown and require further investigations. Herein we show that addition of BCD inhibited the deposition of C1q, ficolin-2 and C3c on CC surface resulting in decreased generation of TCC in plasma, most likely due to competitive binding of BCD to the CC surface (21), thereby preventing complement activation. In plasma from an immunodeficient patient with low IgM and IgA concentration, the deposition of IgA and IgM on CC was reduced, along with an abolished TCC formation in response to CC. This indicates an important role for one or both immunoglobulins in complement activation by CC, and indeed, BCD inhibited the

deposition of IgM and IgA to the CC surface. When comparing BCD and compstatin for inhibition of IgM deposition on CC we found that BCD takes IgM deposition down to background levels, whereas no inhibitory effect was observed with compstatin. Since IgM seems crucial for CC-induced complement activation (Fig. 3F and (11)), we suggest that BCD primarily affects CC-induced complement activation by reducing IgM deposition on CC. Moreover, BCD did not affect formation of TCC by neither mono sodium urate crystals nor zymosan. These data suggest that BCD is a specific inhibitor of CC-induced complement activation.

BCD treatment of human carotid plaques revealed a complex regulation of complement gene expressions (21). The most prominent is the downregulation of mRNA expression of C5 and upregulation of C3, the most central factors of the complement cascade. C3 knock-out mice have been observed to have an enhanced atherosclerotic development and a less beneficial lipid profile than wild type (28) and C3a receptor knock out mice are more prone to severe sepsis development (29), indicating a potential anti-inflammatory role for C3 and its cleavage products and receptors (reviewed in (30)). In contrast, the cleavage product C5a is a potent effector molecule in CC-mediated inflammatory responses (8). In addition, BCD also downregulated MASP-1, C1q A and B chain and factor B which together represent all three pathways indicated to be involved in CC-induced complement activation (8, 11). In line with this, BCD upregulates C1-inhibitor (SERPING1), that inhibits the C1-complex and MASP-1 and -2 (Fig. 8) (21). Together these results indicate a beneficial role of BCD in regulating functions of the complement system in human carotid plaques that may result in reduced inflammation.

Following complement activation, CC are phagocytosed, but in comparison with compstatin, BCD had no reducing effect on phagocytosis of CC. This result suggests that BCD and compstatin inhibit CC-induced complement activation by different mechanisms. When

460 comparing C3c and TCC depositions on CC, BCD was less effective than compstatin in
461 suppressing the deposition of both these complement factors. Thus, complement opsonins
462 may still remain in the presence of BCD that can contribute to phagocytosis of CC. Despite
463 that BCD did not change phagocytosis of CC, it strongly reduced the CC-induced ROS
464 formation in monocytes and granulocytes. BCD also lowered the surface expression of CR3
465 and CR1 on monocytes in response to CC incubation. This was not the case in granulocytes,
466 as is in line with low cytokine release in response to CC in these cells (8). ROS formation,
467 caspase-1 activation, NLRP3 and IL-1β mRNA expression and IL-1β release are events
468 coupled to NLRP3 inflammasome activation by CC (6-8). We observed a reducing effect on
469 CC- induced IL-1β and caspase-1 mRNA expression in PBMC and reduced ROS formation in
470 whole blood. There was also a small, but not significant, reduction in IL-1β release and
471 NLRP3 mRNA expression in PBMC in the presence of BCD. However, the BCD effect was
472 more evident at earlier time points. The weak effect of BCD on NLRP3 mRNA expression
473 may be due to a high basal expression in monocytes compared to macrophages (31), and only
474 a weak upregulation by CC is observed in primed monocytes (8). In addition, BCD by itself
475 significantly reduced caspase-1 activation, however, it only weakly attenuated the CC-
476 induced caspase-1 activation. Furthermore, BCD reduced CC-induced pro-inflammatory
477 cytokine release from PBMC. Gene expression of a range of chemokines and cytokines in
478 PBMC revealed the same pattern, with downregulation of the CC-induced pro-inflammatory
479 cytokines such as IL-1α, IL-1β, IL-6, and a slight non-significant reduction of TNF
480 expression after exposure to BCD. This indicates that BCD is lowering several CC-induced
481 inflammatory responses in human PBMC.

482 In this study, we have focused on upstream activation processes and found that BCD is a
483 potent inhibitor of CC-induced complement activation, which likely contributes to the
484 observed anti-inflammatory effects of BCD, including its effect on the cytokine profile in CC

485 exposed PBMC. BCD seems to have its main effect on reducing IgM deposition on CC, and
486 by this reduce CC-induced complement activation. Moreover, BCD has regulatory effects on
487 complement-related genes in cells from human atherosclerotic plaques which may reduce C5
488 levels, and thereby lowering its cleavage product, C5a, and preventing its potent pro-
489 inflammatory effect. These effects could be beneficial and important for a potential use of
490 BCD for treatment of atherosclerosis.

491

492 **Acknowledgements**

493 We would like to thank Kirsten Krohg Sørensen (Department of Thoracic and Cardiovascular
494 Surgery, Oslo University Hospital Rikshospitalet, Oslo, Norway Oslo University Hospital,
495 Oslo, Norway) for contributing to collection of carotid plaques and Jacob Storgaard Jensen
496 (Storgaard Design) for help with the graphics.

497

498 **Disclosures**

499 The other authors report no conflict.

500 **References**

501 1. Taylor, F. C., M. Huffman, and S. Ebrahim. 2013. Statin therapy for primary
502 prevention of cardiovascular disease. *JAMA* 310: 2451-2452.

503 2. Diamond, D. M., and U. Ravnskov. 2015. How statistical deception created the
504 appearance that statins are safe and effective in primary and secondary prevention of
505 cardiovascular disease. *Expert Rev Clin Pharmacol* 8: 201-210.

506 3. Boekholdt, S. M., G. K. Hovingh, S. Mora, B. J. Arsenault, P. Amarenco, T. R.
507 Pedersen, J. C. LaRosa, D. D. Waters, D. A. DeMicco, R. J. Simes, A. C. Keech, D.
508 Colquhoun, G. A. Hitman, D. J. Betteridge, M. B. Clearfield, J. R. Downs, H. M. Colhoun, A.
509 M. Gotto, Jr., P. M. Ridker, S. M. Grundy, and J. J. Kastelein. 2014. Very low levels of
510 atherogenic lipoproteins and the risk for cardiovascular events: a meta-analysis of statin trials.
511 *J Am Coll Cardiol* 64: 485-494.

512 4. Fitchett, D. H., R. A. Hegele, and S. Verma. 2015. Cardiology patient page. Statin
513 intolerance. *Circulation* 131: e389-391.

514 5. Abela, G. S. 2010. Cholesterol crystals piercing the arterial plaque and intima trigger
515 local and systemic inflammation. *J Clin Lipidol* 4: 156-164.

516 6. Duewell, P., H. Kono, K. J. Rayner, C. M. Sirois, G. Vladimer, F. G. Bauernfeind, G.
517 S. Abela, L. Franchi, G. Nunez, M. Schnurr, T. Espevik, E. Lien, K. A. Fitzgerald, K. L.
518 Rock, K. J. Moore, S. D. Wright, V. Hornung, and E. Latz. 2010. NLRP3 inflammasomes are
519 required for atherogenesis and activated by cholesterol crystals. *Nature* 464: 1357-1361.

520 7. Rajamaki, K., J. Lappalainen, K. Oorni, E. Valimaki, S. Matikainen, P. T. Kovanen,
521 and K. K. Eklund. 2010. Cholesterol crystals activate the NLRP3 inflammasome in human
522 macrophages: a novel link between cholesterol metabolism and inflammation. *PLoS One* 5:
523 e11765.

524 8. Samstad, E. O., N. Niyonzima, S. Nymo, M. H. Aune, L. Ryan, S. S. Bakke, K. T.
525 Lappegard, O. L. Brekke, J. D. Lambris, J. K. Damas, E. Latz, T. E. Mollnes, and T. Espevik.
526 2014. Cholesterol crystals induce complement-dependent inflammasome activation and
527 cytokine release. *J Immunol* 192: 2837-2845.

9. Nidorf, S. M., J. W. Eikelboom, and P. L. Thompson. 2014. Targeting Cholesterol Crystal-Induced Inflammation for the Secondary Prevention of Cardiovascular Disease. *Journal of Cardiovascular Pharmacology and Therapeutics* 19: 45-52.

10. Torzewski, M., and S. Bhakdi. 2013. Complement and atherosclerosis-united to the point of no return? *Clin Biochem* 46: 20-25.

11. Pilely, K., A. Rosbjerg, N. Genster, P. Gal, G. Pal, B. Halvorsen, S. Holm, P. Aukrust, S. S. Bakke, B. Sporsheim, I. Nervik, N. Niyonzima, E. D. Bartels, G. L. Stahl, T. E. Mollnes, T. Espevik, and P. Garred. 2016. Cholesterol Crystals Activate the Lectin Complement Pathway via Ficolin-2 and Mannose-Binding Lectin: Implications for the Progression of Atherosclerosis. *J Immunol*.

12. Lappegard, K. T., P. Garred, L. Jonasson, T. Espevik, P. Aukrust, A. Yndestad, T. E. Mollnes, and A. Hovland. 2014. A vital role for complement in heart disease. *Mol Immunol* 61: 126-134.

13. Barratt-Due, A., S. E. Pischke, P. H. Nilsson, T. Espevik, and T. E. Mollnes. 2016. Dual inhibition of complement and Toll-like receptors as a novel approach to treat inflammatory diseases-C3 or C5 emerge together with CD14 as promising targets. *J Leukoc Biol*.

14. Loftsson, T., P. Jarho, M. Másson, and T. Järvinen. 2005. Cyclodextrins in drug delivery. *Expert Opinion on Drug Delivery* 2: 335-351.

15. Brady, R. O., M. R. Filling-Katz, N. W. Barton, and P. G. Pentchev. 1989. Niemann-Pick disease types C and D. *Neurol Clin* 7: 75-88.

16. Taylor, A. M., B. Liu, Y. Mari, B. Liu, and J. J. Repa. 2012. Cyclodextrin mediates rapid changes in lipid balance in Npc1−/− mice without carrying cholesterol through the bloodstream. *Journal of Lipid Research* 53: 2331-2342.

17. Matsuo, M., M. Togawa, K. Hirabaru, S. Mochinaga, A. Narita, M. Adachi, M. Egashira, T. Irie, and K. Ohno. 2013. Effects of cyclodextrin in two patients with Niemann-Pick Type C disease. *Mol Genet Metab* 108: 76-81.

18. Gould, S., and R. C. Scott. 2005. 2-Hydroxypropyl-beta-cyclodextrin (HP-beta-CD): a toxicology review. *Food Chem Toxicol* 43: 1451-1459.

19. Stella, V. J., and Q. He. 2008. Cyclodextrins. *Toxicol Pathol* 36: 30-42.

20. Brewster, M. E., K. S. Estes, and N. Bodor. 1990. An Intravenous Toxicity Study of 2-Hydroxypropyl-Beta-Cyclodextrin, a Useful Drug Solubilizer, in Rats and Monkeys. *International Journal of Pharmaceutics* 59: 231-243.

21. Zimmer, S., A. Grebe, S. S. Bakke, N. Bode, B. Halvorsen, T. Ulas, M. Skjelland, D. De Nardo, L. I. Labzin, A. Kerksiek, C. Hempel, M. T. Heneka, V. Hawxhurst, M. L. Fitzgerald, J. Trebicka, I. Bjorkhem, J. A. Gustafsson, M. Westerterp, A. R. Tall, S. D. Wright, T. Espevik, J. L. Schultze, G. Nickenig, D. Lutjohann, and E. Latz. 2016. Cyclodextrin promotes atherosclerosis regression via macrophage reprogramming. *Sci Transl Med* 8: 333ra350.

22. Qu, H., D. Ricklin, H. Bai, H. Chen, E. S. Reis, M. Maciejewski, A. Tzekou, R. A. DeAngelis, R. R. Resuello, F. Lupu, P. N. Barlow, and J. D. Lambris. 2013. New analogs of the clinical complement inhibitor compstatin with subnanomolar affinity and enhanced pharmacokinetic properties. *Immunobiology* 218: 496-505.

23. Munthe-Fog, L., T. Hummelshoj, B. E. Hansen, C. Koch, H. O. Madsen, K. Skjodt, and P. Garred. 2007. The impact of FCN2 polymorphisms and haplotypes on the Ficolin-2 serum levels. *Scand J Immunol* 65: 383-392.

24. Rosbjerg, A., N. Genster, K. Pilely, M. O. Skjoedt, G. L. Stahl, and P. Garred. 2016. Complementary Roles of the Classical and Lectin Complement Pathways in the Defense against Aspergillus fumigatus. *Front Immunol* 7: 473.

25. Mollnes, T. E., O. L. Brekke, M. Fung, H. Fure, D. Christiansen, G. Bergseth, V. Videm, K. T. Lappegard, J. Kohl, and J. D. Lambris. 2002. Essential role of the C5a receptor in E coli-induced oxidative burst and phagocytosis revealed by a novel lepirudin-based human whole blood model of inflammation. *Blood* 100: 1869-1877.

26. Bergseth, G., J. K. Ludviksen, M. Kirschfink, P. C. Giclas, B. Nilsson, and T. E. Mollnes. 2013. An international serum standard for application in assays to detect human complement activation products. *Mol Immunol* 56: 232-239.

584 27. Daha, M. R., and C. van Kooten. 2016. Role of complement in IgA nephropathy. *J*
585 *Nephrol* 29: 1-4.

586 28. Persson, L., J. Boren, A. K. Robertson, V. Wallenius, G. K. Hansson, and M. Pekna.
587 2004. Lack of complement factor C3, but not factor B, increases hyperlipidemia and
588 atherosclerosis in apolipoprotein E-/- low-density lipoprotein receptor-/- mice. *Arterioscler*
589 *Thromb Vasc Biol* 24: 1062-1067.

590 29. Kildsgaard, J., T. J. Hollmann, K. W. Matthews, K. Bian, F. Murad, and R. A. Wetsel.
591 2000. Cutting edge: targeted disruption of the C3a receptor gene demonstrates a novel
592 protective anti-inflammatory role for C3a in endotoxin-shock. *J Immunol* 165: 5406-5409.

593 30. Coulthard, L. G., and T. M. Woodruff. 2015. Is the complement activation product
594 C3a a proinflammatory molecule? Re-evaluating the evidence and the myth. *J Immunol* 194:
595 3542-3548.

596 31. Guarda, G., M. Zenger, A. S. Yazdi, K. Schroder, I. Ferrero, P. Menu, A. Tardivel, C.
597 Mattmann, and J. Tschopp. 2011. Differential expression of NLRP3 among hematopoietic
598 cells. *J Immunol* 186: 2529-2534.

599

Figure legends

Figure 1. BCD inhibits CC-induced complement activation. (A) Full complement activation was evaluated in human plasma incubated with or without BCD (5 or 10mM), and incubated with CC (0.5 or 1 mg/ml), MSU (0.25 mg/ml), HSA/PBS or Zym-IgG (10 μg/ml) for 30 min. The end product in complement activation, TCC, is considered a measure of full complement activation. Data is shown as mean+SEM, n = 9 healthy donors, *$p<0.05$, **$p<0.01$ vs PBS/HSA or as otherwise indicated. (B-C) Binding of TCC or C3c on the CC was determined in human plasma incubated with CC with or without 10 mM BCD or 20 μM compstatin for 30 min. The isotype control is shown in light grey, filled. (B) Deposition of TCC on the crystals, with (dashed line) or without (black solid line) the presence of BCD, and with the presence of compstatin (dotted line) was detected using an anti-C5b-9 and the secondary antibody was Alexa Fluor-488. (C) Deposition of C3c on the crystals, with (dashed line) or without (black solid line) the presence of BCD, and with the presence of compstatin (dotted line) was stained with a FITC conjugated antibody against C3c. Data shown are one representative of three independent experiments, n=3 healthy donors. AU: arbitrary units, BCD: 2-hydroxypropyl-β-cyclodextrin, C3c: complement factor c, CC: cholesterol crystals, MSU: monosodium urate crystals, TCC; terminal complement complex, Zym: Zymosan.

Figure 2. BCD prevents deposition of complement recognition molecules on the CC surface. (A-D) Human plasma or serum was incubated with CC with or without 10 mM BCD for 30 min. (A-B) C1q and ficolin-2 deposition on CC with (dashed line) or without (black solid line) the presence of BCD was stained in plasma with anti-C1q and anti-ficolin-2, and the secondary antibodies were PE and Alexa Fluor-488, respectively. Data shown are one representative of three independent experiments, n=3 healthy donors. Isotype control is light

grey, filled. (C-D) Human serum was incubated with CC with or without 10 mM BCD, C1q (10 μg/ml) or ficolin-2 (10 μg/ml) blocking antibodies for 30 min. C1q and ficolin-2 deposition on CC was stained in plasma with anti-C1q and anti-ficolin-2, and the secondary antibodies were PE and Alexa Fluor-488, respectively. Isotype control is white, filled. Control antibody for the blocking antibodies is shown as indicated. Data shown are mean + SEM, n=3 healthy donors, ****$p<0.0001$ vs PBS or as otherwise indicated. BCD: 2-hydroxypropyl-β-cyclodextrin, C1q: complement factor 1q, CC: cholesterol crystals.

Figure 3. IgA and IgM binding to CC are essential for CC-induced complement activation. (A-E) Deposition of Ig on the crystals was determined in plasma incubated with CC for 30 min. The isotype controls are presented as light grey, filled. Data shown are one representative of three independent experiments, n=3 healthy donors. (A) IgG binding to CC detected using a PE conjugated antibody against IgG (black solid line). (B) IgM deposition on CC detected using a FITC conjugated antibody against IgM (dotted) or IgGAM (mixture of IgG, IgA and IgM, black solid line). (C) IgA binding to CC detected using a FITC conjugated monoclonal antibody to IgA (dashed) or IgGAM (mixture of IgG, IgA and IgM, black solid line). (D-E) Deposition of IgM or IgA on the CC was determined in human healthy plasma (dotted), or plasma from a patient with common variable immunodeficiency (CVID) with (black solid line) or without (dashed) reconstitution with pentaglobin. IgA and IgM binding to CC were detected using a FITC conjugated monoclonal antibody. (F) TCC formation in human healthy plasma or plasma from a patient with common variable immunodeficiency (CVID) that was incubated with HSA, CC (1 mg/ml) or Zym-IgG (10 μg/ml) for 30 min. Data is shown as mean+SEM of three independent experiments (n = 1 patient, n= 3 healthy donors). AU: arbitrary units, BCD: 2-hydroxypropyl-β-cyclodextrin, CC: cholesterol crystals, TCC; terminal complement complex, Zym: Zymosan.

Figure 4. BCD prevents deposition of IgA and IgM on the CC surface. (A-C) Human plasma was incubated with CC with or without BCD (10 mM) for 30 min. Deposition of IgGAM (mixture of IgG, IgA and IgM), IgM and IgA on the crystals, with (dashed line) or without (black solid line) BCD was determined by staining with FITC conjugated antibody against IgM, IgGAM or IgA. The isotype control is presented as light grey, filled. Data shown are one representative of three independent experiments, n=3 healthy donors. BCD: 2-hydroxypropyl-β-cyclodextrin, CC: cholesterol crystals.

Figure 5. BCD reduces CC-induced upregulation of complement receptors CR3 and CR1 in monocytes. (A-F) CC (1 mg/ml) were pre-incubated with BCD (10 mM), compstatin (20 μM) or PBS for 15 min, before incubation with whole blood for 30 min. (A, B) Phagocytosis of CC was determined based on side scatter signal shift after CC ingestion by monocytes and granulocytes, presented as percentage of cells with CC. Median fluorescent intensity (MFI) of CR3 (C, D) and CR1 (E, F) on monocytes and granulocytes were measured. Data shown are mean +/- SEM for n= 6 healthy donors, *$p<0.05$ vs CC. BCD: 2-hydroxypropyl-β-cyclodextrin, CC: cholesterol crystals, CR: complement receptor, MFI: Mean fluorescence intensity.

Figure 6. BCD inhibits CC-induced ROS formation and reduces Caspase-1 activation. CC (1 mg/ml) or PBS were pre-incubated with BCD (10 mM), compstatin (20 μM) or PBS for 15 min before incubation with whole blood for 10 min. (A-B) ROS production is shown as a percentage of DHR 123 in monocytes or granulocytes in whole blood. (C-D) Activation of caspase-1 was detected as percentage of FLICA in monocytes or granulocytes in whole blood. Data shown are mean +/- SEM for n= 9 healthy donors, *$p<0.05$ vs PBS or as otherwise

673 indicated. BCD: 2-hydroxypropyl-β-cyclodextrin, CC: cholesterol crystals, DHR:
674 dihydrorhodamine, ROS: Reactive oxygen species.

675

676 Figure 7. BCD modifies CC-induced expression of cytokines and cytokine-related genes and
677 reduces cytokine release in PBMC. (A-B) PBMC were isolated from whole blood and
678 preincubated with BCD (10 mM) for 1 h, then incubated with CC (2 mg/ml) for 5h in 50 %
679 autologous plasma. (A) mRNA profiling with nCounter Analysis system with probes from
680 nCounter GX Human Immunology kit. Presented cytokines, chemokines and related genes
681 with p-values and fold change for the comparison CC+BCD vs CC, n= 9 healthy donors.
682 Genes were that were changed $p<0.05$ and/or $-2<\text{fold change}>2$ are presented with gene
683 names. (B) Cytokines and chemokines were quantified in plasma by multiplex assay, n = 6-9
684 healthy donors. CC induced the release of IL-1β, IL-6, IL1α, MIP-1α ($p<0.05$) and TNF
685 ($p<0.001$), and BCD reduced the CC-induced release of IL-6, IL1α, MIP-1α ($p<0.05$), IL8
686 and TNF ($p<0.001$). Data are presented as fold change normalized to PBS. Raw data (mean ±
687 SEM) are presented in Supplemental Table 1. BCD: 2-hydroxypropyl-β-cyclodextrin, CC:
688 cholesterol crystals.

689

690 Figure 8. BCD affects the gene expression of genes involved in complement system in human
691 carotid plaques. Carotid plaques were treated with or without BCD for 16 h ex vivo, RNA
692 isolated and samples run on nCounter Analysis system with probes from nCounter GX
693 Human Immunology kit spiked with 30 selected genes. Presented are the genes involved in
694 the complement cascade with fold change indicated as upregulated (red) or downregulated
695 (blue) with BCD treatment visualized in Adobe Illustrator for n=10 carotid arteries. In grey
696 are genes not measured or detected. BCD: 2-hydroxypropyl-β-cyclodextrin, C: complement

component, CR: complement receptor, DAF: decay accelator factor/CD55, Fico-2: ficolin-2, Inh: inhibitor, F: complement factor, Cl: clusterin, MASP: MBL-associated serine protease, MBL: Mannose-binding lectin, MCP: membrane-cofactor protein/CD46, TCC: terminal

700 complement complex.

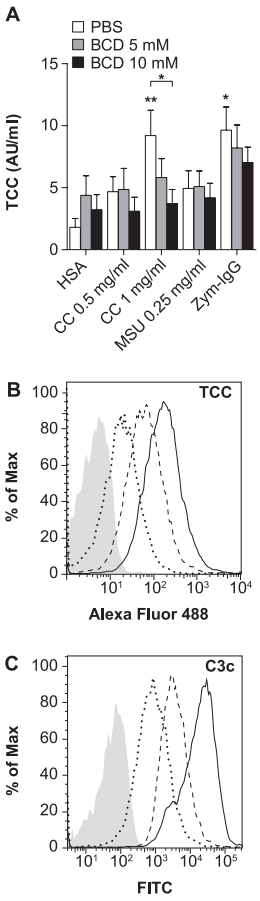

Figure 1

701

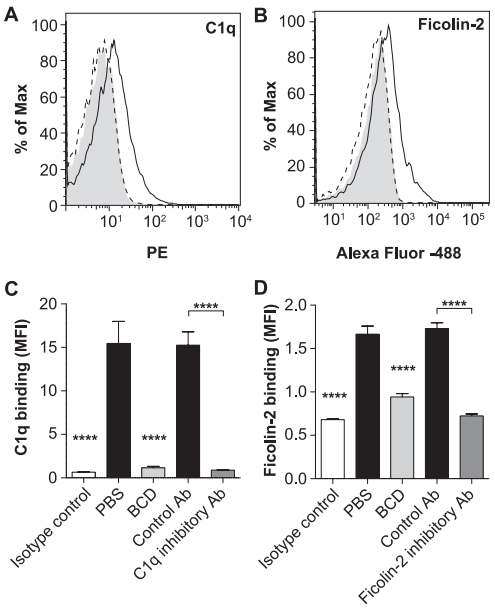
A
C1q
% of Max
PE
B
Ficolin-2
% of Max
Alexa Fluor -488
C
C1q binding (MFI)
****
Isotype control
PBS
BCD
Control Ab
C1q inhibitory Ab
D
Ficolin-2 binding (MFI)
Isotype control
PBS
BCD
Control Ab
Ficolin-2 inhibitory Ab

Figure 2

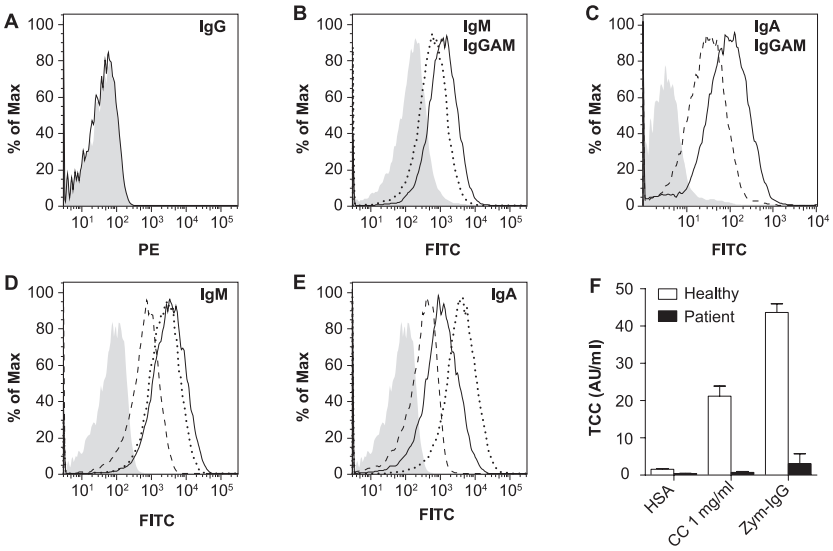
A
IgG
% of Max
PE
B
IgM
IgGAM
FITC
C
IgA
IgGAM
FITC
D
IgM
FITC
E
IgA
FITC
F
Healthy
Patient
TCC (AU/ml)
HSA
CC 1 mg/ml
Zym-IgG

Figure 3

703

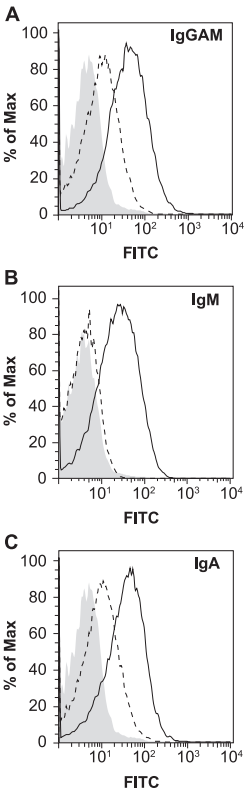

Figure 4

704

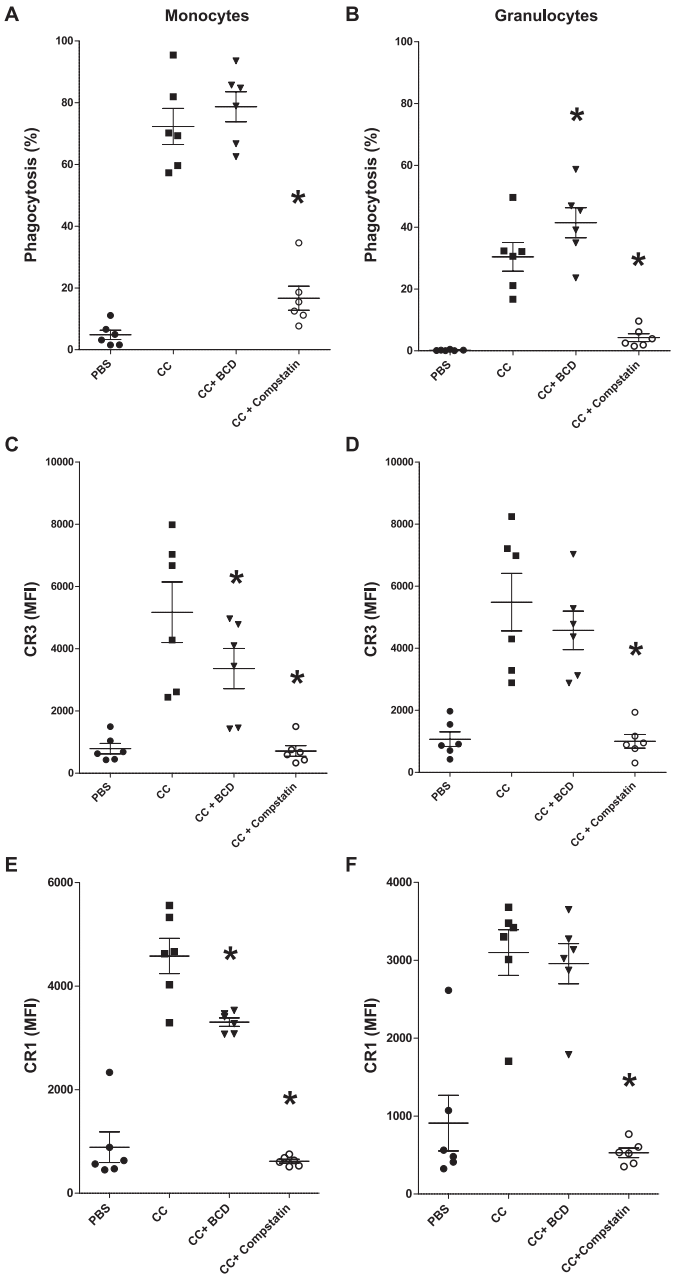
A
Monocytes
Phagocytosis (%)
B
Granulocytes
Phagocytosis (%)
C
CR3 (MFI)
D
CR3 (MFI)
E
CR1 (MFI)
F
CR1 (MFI)
PBS
CC
CC+ BCD
CC+ Compstatin
CC+Compstatin

Figure 5

705

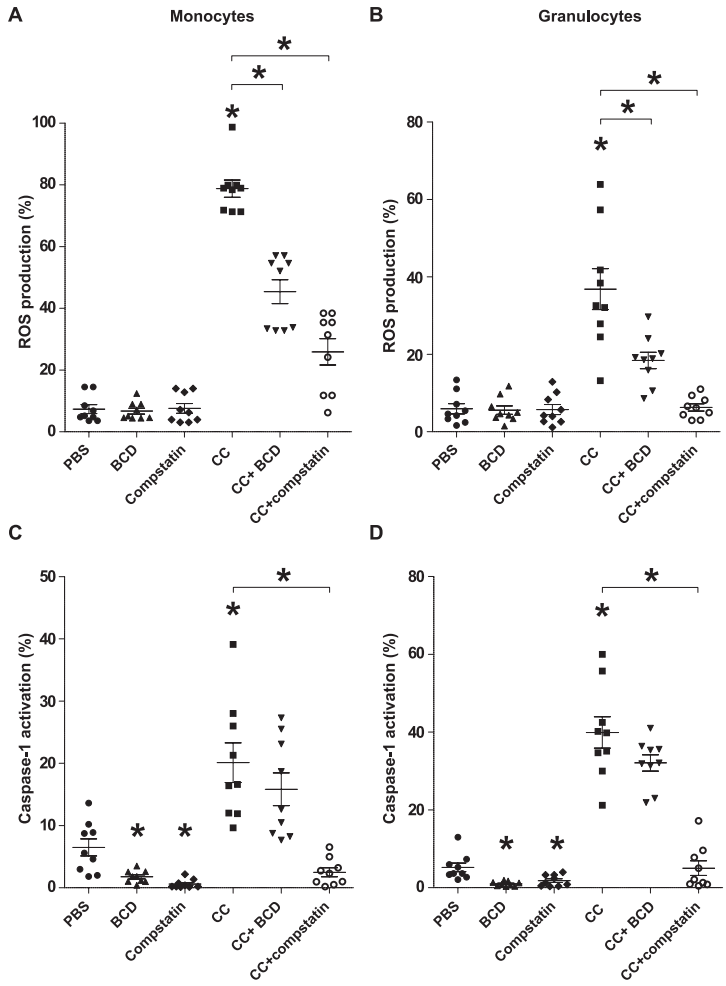
A
Monocytes
B
Granulocytes
ROS production (%)
Caspase-1 activation (%)
PBS
BCD
Compstatin
CC
CC+ BCD
CC+compstatin
C
D

Figure 6

706

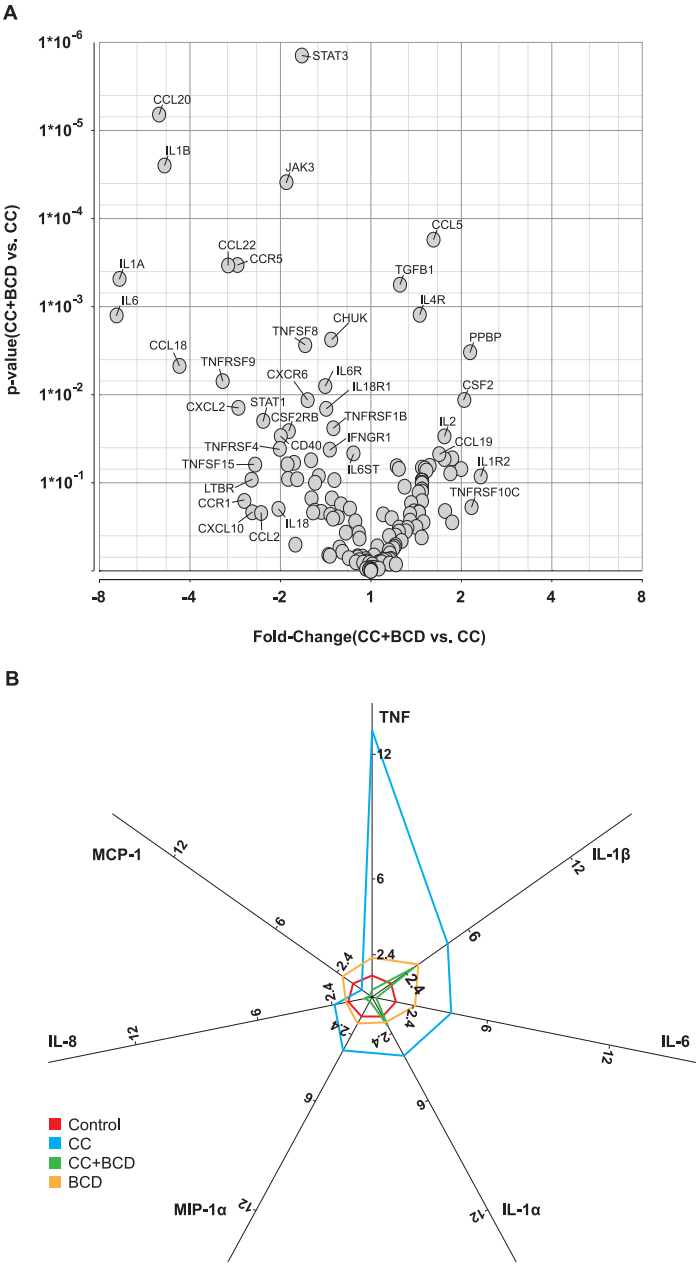
A
p-value(CC+BCD vs. CC)
1*10-6
1*10-5
1*10-4
1*10-3
1*10-2
1*10-1
STAT3
CCL20
IL1B
JAK3
CCL5
CCL22
CCR5
IL1A
TGFB1
IL6
IL4R
CHUK
TNFSF8
PPBP
CCL18
TNFRSF9
CXCR6
IL6R
IL18R1
CSF2
CXCL2
STAT1
CSF2RB
TNFRSF1B
IL2
TNFRSF4
CD40
IFNGR1
CCL19
TNFSF15
IL6ST
IL1R2
LTBR
TNFRSF10C
CCR1
CXCL10
IL18
CCL2
-8
-4
-2
1
2
4
8
Fold-Change(CC+BCD vs. CC)
B
TNF
MCP-1
IL-1β
IL-8
IL-6
MIP-1α
IL-1α
Control
CC
CC+BCD
BCD

Figure 7

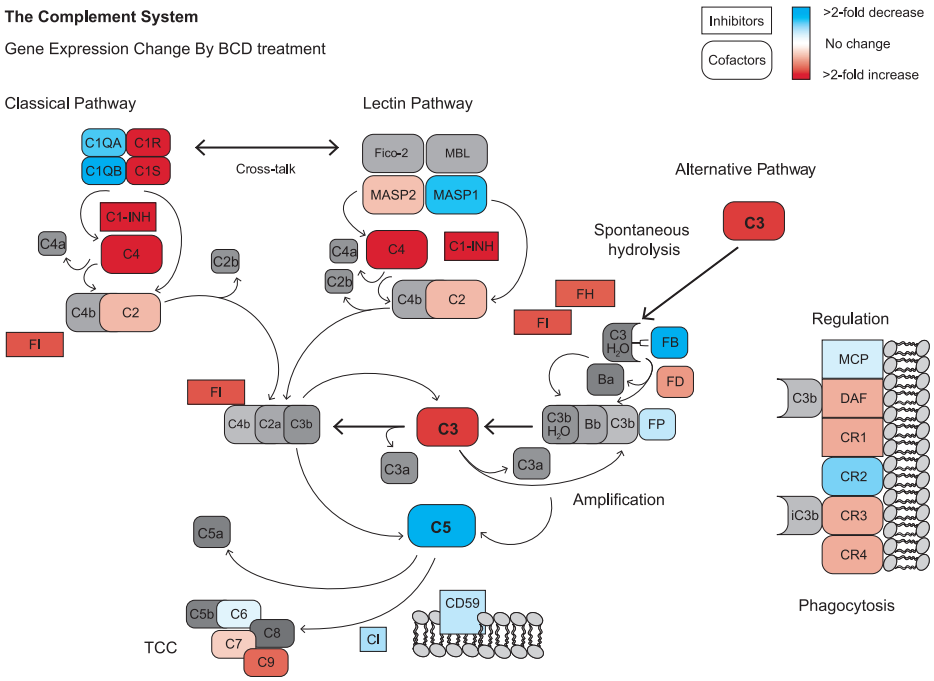
The Complement System
Gene Expression Change By BCD treatment
Inhibitors
Cofactors
>2-fold decrease
No change
>2-fold increase
Classical Pathway
Lectin Pathway
Alternative Pathway
C1QA
C1R
C1QB
C1S
Cross-talk
Fico-2
MBL
MASP2
MASP1
C1-INH
C4a
C4
C2b
C4b
C2
FI
FH
Spontaneous hydrolysis
C3
FB
Ba
FD
C3b
Bb
FP
C3a
Amplification
C5
C5a
C5b
C6
C7
C8
C9
TCC
CI
CD59
Regulation
MCP
DAF
CR1
CR2
CR3
CR4
iC3b
Phagocytosis

Figure 8

708